

Anticorrosive potential of ethanol extract of *Delonix elata* for mild steel in 0.5 M H₂SO₄ - a green approach

D. Mahalakshmi^{1a}, C. B. N. Unnisa¹, V. Hemapriya¹, E. P. Subramaniam², S. M. Roopan³, S. Chitra¹, I.-M. Chung^{4a}, S.-H. Kim⁴, M. Prabakaran^{4*}

¹Department of Chemistry, PSGR Krishnammal College for women, Coimbatore, India

²Department of Chemistry, Coimbatore institute of Technology, Coimbatore, India

³Chemistry of Heterocycles & Natural Product Research Laboratory, Department of Chemistry, School of Advanced Sciences, VIT University, Vellore, India

⁴Department of Crop Science, College of Sanghuh Life Science, Konkuk University, Seoul 05029, South Korea

Received July 16, 2018; Revised August 30, 2018

The phytochemical constituents of *Delonix elata*, characterized by gas chromatography-mass spectroscopy (GC-MS) and their inhibitive action on mild steel in 0.5 M H₂SO₄ medium, are discussed in the present study. The impedance and polarization techniques showed a similar trend as regards concentration and inhibition efficiency. The optimized concentration of *D. elata* (10 % v/v) resulted in high inhibition efficiency (85.96%). To confirm the adsorption of inhibitors on the mild steel surface, morphological studies of the latter were carried out by means of scanning electron microscopy (SEM), energy dispersive spectroscopy (EDX) and atomic force microscopy (AFM) techniques for both uninhibited and inhibited specimens. The electrochemical measurements and surface studies were well associated with each other.

Keywords: *Delonix elata*, GC-MS, Inhibitive action, SEM-EDX-AFM

INTRODUCTION

The supreme properties of metals and alloys have gained vast attention from earlier days. Among the existing metals, low cost and remarkable functional properties of iron and its alloys had made it to enter the construction fields and industrial sectors [1]. The extent of its usage in industrial sectors without proper remedial measures leads to huge economical loss. In specific, mild steel is extensively used in various fields such as construction, automobile, petroleum and oil industries due to its low cost and excellent mechanical strength [2, 3]. When such metal is subjected to pickling, cleaning and descaling processes [4] in presence of mineral acids like hydrochloric acid and sulphuric acid, undoubtedly base metal dissolution takes place in addition to the removal of oxide coatings and corrosion products. Such deterioration of metals is a serious problem which should be taken care of to find a solution to minimise the loss where complete elimination is impossible. As a remedy, usage of inhibitors is a low-cost method which can slow down or prevent the metal loss when added in acid solutions [5]. In this regard, organic inhibitors have gained long-term attention in minimising the corrosion rate to the maximum extent due to their heteroatoms such as S, O and N and their π electron density, which could behave as adsorption centres. Though the organic compounds are acknowledged with good

inhibition efficiency, their cost, synthetic methodology and toxicity limit their usage [6]. Thus, recent researches are turning towards exploring the green and eco-friendly corrosion inhibitors originating from plant sources. The plant extracts, boosted with phytochemical constituents such as amino acids, terpenoids, flavonoids, alkaloids, polyphenols, tannins, etc., along with their simple preparative methods, low cost, easy availability and renewable resources, are environmentally acceptable ones [7]. To strengthen the platform of green inhibitors, lot of research work has been carried out by various researchers using different plant sources as corrosion reducers for different metals in various aggressive media, which is evident from the reports documented using extracts of watermelon rind [8], *Justicia gendarussa* [9], *Ligularia fischeri* [10], *Phyllanthus amarus*, *Oxandra asbeckii*, *Phyllanthus amarus* [11], *Zenthoxylum alatum* [12], *Tragia plukenetii* [13], *Tripleurospermum auriculatum*, *Teucrium oliverianum* [14], *Silybum marianum* [15], *Egyptian licorice* [16], *Ginkgo biloba* [17], etc. In order to highlight the potential of green inhibitors, in the present work *Delonix elata* was chosen, a hermaphroditic, deciduous tree originating from Caesalpinioideae family. Its leaves and barks are widely used in Siddha and Ayurveda. It is known for its anti-inflammatory [18], anti-rheumatic, anti-microbial [19] and antioxidant [20] activities. As reported by Singh *et al.* [21], leaf extracts of

* To whom all correspondence should be sent:

E-mail: prabakaranitt@gmail.com;
prabakaran@konkuk.ac.kr

^aD. Mahalakshmi and I.-M. Chung have equally contributed to this work.

Delonix elata were found to possess active ingredients like tannins, saponins, quinones, terpenoids, steroids, flavonoids, phenols, alkaloids and coumarins. Its active ingredients rich in heteroatoms and aromaticity are expected to provide good protection for metals. In order to check this expectation, an ethanol extract of leaves of *Delonix elata* was prepared to study its inhibition efficiency for mild steel in 0.5 M H₂SO₄ medium using electrochemical and non-electrochemical techniques. Surface characterization studies were made by SEM, EDX, and AFM analysis and are discussed in the forthcoming sections.

EXPERIMENTAL METHODS

The mild steel samples were machined in to appropriate dimensions of 3 × 1 × 1 cm followed by pickling with hydrochloric acid to remove impurities. The samples were abraded with various grades of emery sheets for polished surface and stored in a desiccator for further usage. The electrolytic solution of 0.5 M H₂SO₄ was prepared with double distilled water. The leaves of *Delonix elata* were collected, washed several times with double distilled water, shade dried and finally made into powder. About 1 g of powder was allowed to reflux with 100 ml of ethanol for 3 h. Later the cooled extract was filtered and refrigerated for further use.

Gas chromatography-mass spectroscopy (GC-MS)

The required amount of sample was diluted with ethanol and was analyzed by GC-MS using Perkin Elmer Clarus 60 instrument equipped with a DB 5-MS capillary standard non-polar column (30 m × 0.25 i.d., film thickness 0.25 μm). An electron ionization system with 70 eV ionization energy was used for the detection of components along with helium gas (99.999 % purity), and operating parameters like sample volume (1 μL), delay time (2 min) and running time (40 min).

Electrochemical measurements

An electrochemical work station, IVIUM compactstat potentiostat/galvanostat was used. The measurements were carried out in a three-electrode cell assembly comprising a mild steel rod of 0.785 cm² exposure, platinum and calomel electrode as working, counter and reference electrodes. The open circuit potential (OCP) was measured after stabilizing the system. An electrochemical impedance spectroscopy (EIS) test was carried out in the frequency range of 10 KHz to 0.01 Hz using superimposed sine wave amplitude of 10 mV. From the plots obtained for the selected concentrations of the inhibitors (2, 6 and 10 % v/v), impedance

parameters like charge transfer resistance (R_{ct}) and constant phase element (CPE) for uninhibited and extract-inhibited medium were sorted from which inhibition efficiency was calculated using the equation below:

$$\text{Inhibition efficiency(\%)} = \frac{R_{ct(\text{inh})} - R_{ct(\text{Blank})}}{R_{ct(\text{inh})}} \times 100 \quad (1)$$

where, R_{ct(inh)} and R_{ct(Blank)} are the charge transfer resistances of inhibited and uninhibited samples, respectively. Followed by impedance measurements, potentiodynamic polarization measurements were carried out by applying a potential range of -200 mV to +200 mV at a scan rate of 1 mV/sec under similar experimental set up. From the resulting Tafel plots, polarization parameters like corrosion current (I_{corr}), corrosion potential (E_{corr}) and Tafel slopes (b_a and b_c) were drawn:

$$\text{Inhibition efficiency(\%)} = \frac{I_{\text{corr}(\text{blank})} - I_{\text{corr}(\text{inh})}}{I_{\text{corr}(\text{blank})}} \times 100 \quad (2)$$

where, I_{corr(blank)} and I_{corr(inh)} correspond to the corrosion current of uninhibited and inhibited medium, respectively.

Surface analysis (SEM-EDX and AFM)

The extent of a metal to undergo corrosion in uninhibited and inhibited (10 % v/v) medium can be additionally evidenced by SEM analysis. The elemental composition of the samples can be retrieved from the EDX analysis. SEM analysis coupled with EDX was done with a biomedical research microscope (Mumbai, India). Multimode scanning probe microscope (NTMDT, NTEGRA prima, Russia) with cantilever length, width and thickness of 135, 30 and 2 μm, respectively and 0.35-6.06 N/m force constant assisted with NOVA software was used to record the AFM images for both inhibited and uninhibited samples.

RESULTS AND DISCUSSION

Gas chromatography-mass spectroscopy (GC-MS)

Fig. 1 shows the GC-MS spectra representing the phytochemical constituents of the ethanol extract of *Delonix elata*. Fig. 2a shows the structure of 9 major peaks (based on their retention times) corresponding to the phytoconstituents: a) propane-1-1-3-triethoxy (RT=5.40), b) DL-homocystine (RT = 7.64), c) melezitose (RT=10.76), d) l-(+)-ascorbic acid 2,6-dihexadecanoate (RT=21.48), e) 1,2,3,4-tetrahydro-N-(1-methylethyl)-N-(phenylmethyl) 2-naphthalenamine, (RT=24.29), f) L-ascorbic acid-6-octadecanoate (RT=25.2), g) 1-vinyl-1-hydroxycholestane (RT=30.18), h) 2-(3-acetoxy-4,4,14-trimethylandro-8-en-17-yl) propanoic acid

D. Mahalakshmi et al.: Anticorrosive potential of ethanol extract of *Delonix elata* for mild steel in 0.5 M H₂SO₄ ... (RT=33.55) and i) 9-hexadecenoic acid eicosyl ester (Z) (RT=35.95). On the other hand, the presence of smaller peaks could be due to small quantities of disintegrated major components. Fig. 2b shows the major components of the extract. Similarly, compounds elicited at lower retention time could be low-polar plant constituents. It is worth noting that all 9 compounds shown in Fig. 2a are a mixture of organic moieties containing O, N

or π -electrons [22], electron-rich multiple bonds [23] which is a necessary criterion for the present discussion. Since the retention times of the majority of the compounds are close to each other and owing to the complex hetero systems, it is difficult to reveal individual actions rendered by the phytoconstituents. Thus, the ethanol extract was used as such for the forthcoming studies.

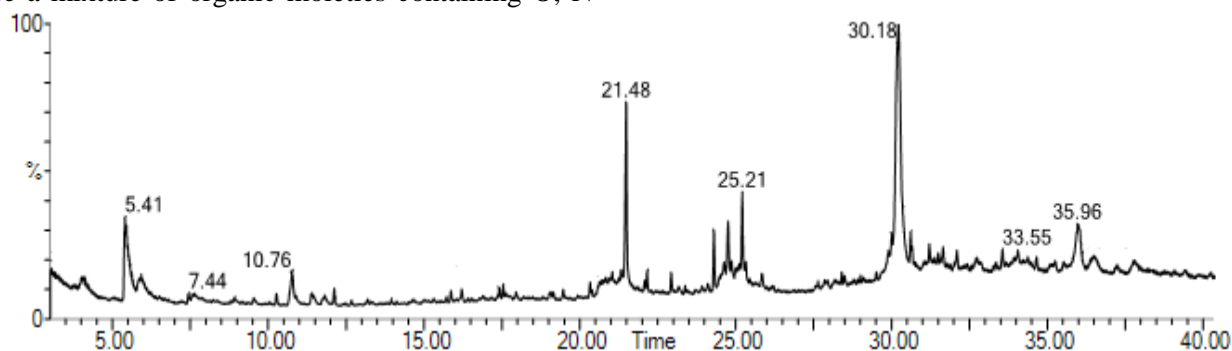


Fig. 1. GC-MS chromatogram of *Delonix elata*.

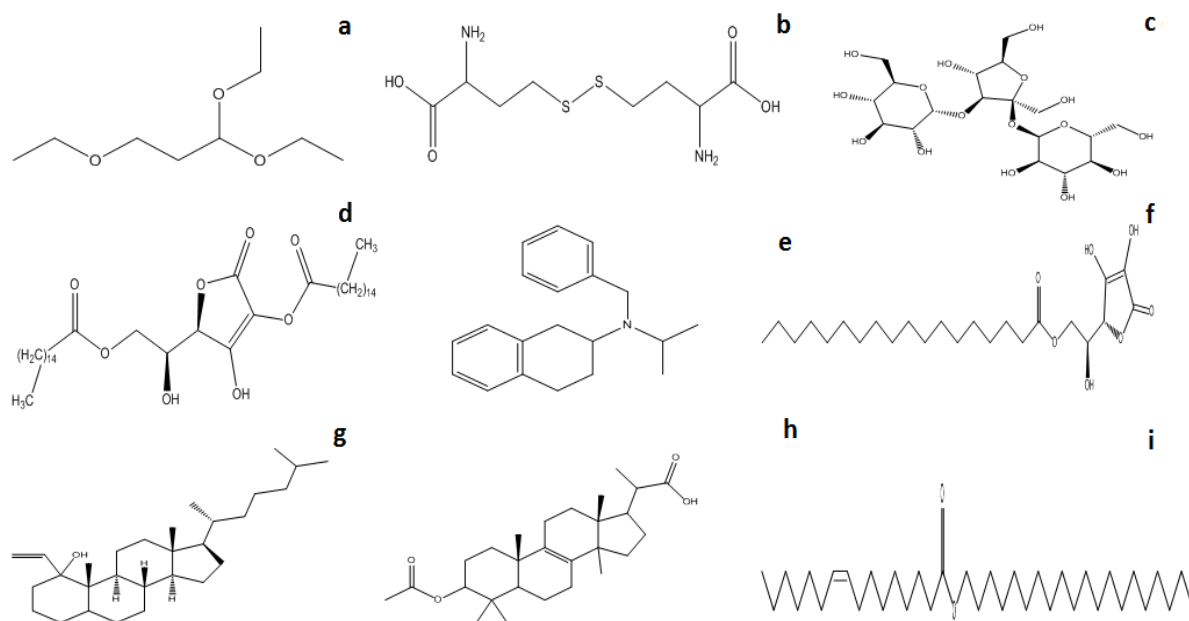


Fig. 2a) Structures of the major phytoconstituents elucidated by GC-MS.

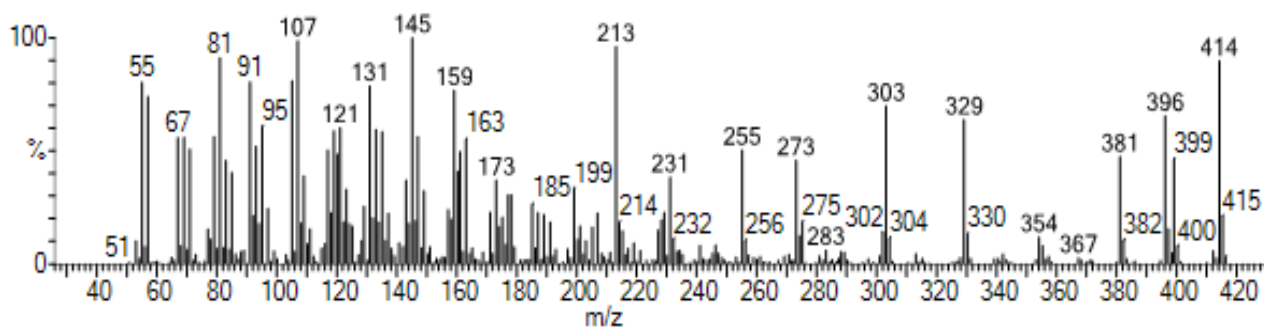


Fig. 2b. Mass spectrum of 1-vinyl-1-hydroxycholestane.

Electrochemical impedance spectroscopy (EIS)

The electrochemical response and reactivity of metal specimens in 0.5 M H₂SO₄ medium was measured after attaining steady-state potential, represented in the form of open circuit potential (OCP). Fig. 3 shows the OCP image of selected concentrations (2, 6, 10 % v/v) of the inhibited test medium.

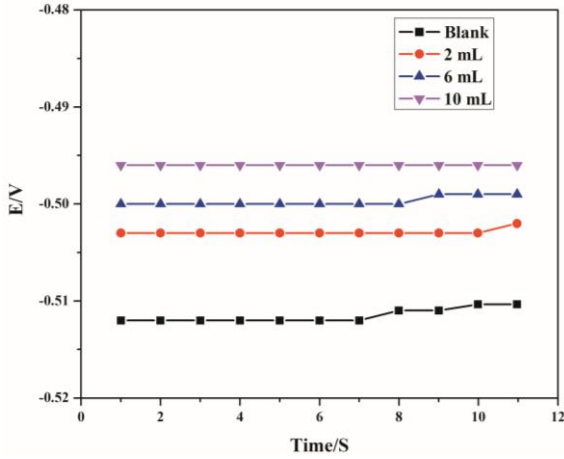


Fig. 3. OCP measurement of the corrosion of mild steel in 0.5 M H₂SO₄.

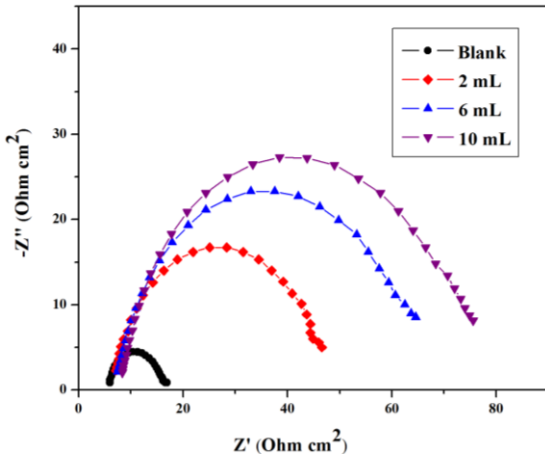


Fig. 4. Nyquist plots for the corrosion of mild steel in 0.5 M H₂SO₄.

From the OCP image, the adsorption of inhibitors on the mild steel surface is evidenced by the shift towards negative potential in presence of inhibitors with reference to uninhibited medium [24, 25]. The EIS technique is a most powerful tool to understand the reactions occurring at the electrochemical interface leading to the adsorption of inhibitor molecules [26]. The EIS measurements for the selected concentrations of inhibitors are reflected in the form of Nyquist plots, as displayed in Fig. 4. The impedance response for the uninhibited and inhibited systems is exhibited in the form of single depressed capacitive loops owing to the fact that the corrosion process on the mild steel

surface is controlled by charge transfer [27]. However, the imperfection in semicircle would be attributed to the inhomogeneity or roughness of the metal surface. On increasing the concentration of the ethanol extract of *Delonix elata* as 2, 6, 10 % v/v, a successive increase in the diameter of the semicircles [28] was found compared to that of uninhibited test medium thereby retaining the shape of the loops [29], suggesting a similar mechanism. This could be correlated with the charge transfer resistance (R_{ct}) values displayed in Table 1.

Table 1. AC-impedance parameters for corrosion of mild steel for selected concentrations of the inhibitors in 0.5 M H₂SO₄.

C % (v/v)	R_{ct} (ohm cm ²)	CPE (μF/cm ²)	IE (%)
Blank	10.12	22.4	-
2	46.98	14.8	78.46
6	63.90	13.7	84.16
10	72.09	12.7	85.96

Table 2. Corrosion parameters for corrosion of mild steel with selected concentrations of the inhibitors in 0.5 M H₂SO₄ by potentiodynamic polarization method.

C % (v/v)	Tafel slopes (mV/dec)		$-E_{corr}$ (mV)	I_{corr} (μA/cm ²)	IE (%)
	b_a	b_c			
Blank	83	139	471	850	-
2	78	145	489.5	477	43.88
6	71	168	482.1	311	63.41
10	66	185	478.8	268	68.47

The increased R_{ct} values from 10.12 Ohm cm² (Blank) to 72.09 Ohm cm² (10 % v/v) reveal the formation of a layer on the metal surface by the phytoconstituents of the added extract thereby retarding the dissolution of metal in acid medium. On the other hand, decreased constant phase element (CPE) from 22.4 (uninhibited) to 12.7 μF/cm² (inhibited) due to the decrease in local dielectric constant or replacement of already adsorbed ions by the added inhibitor molecules or decreased thickness of double layer [30, 31] also suggested the formation of a barrier at the metal/solution interface. The constant phase element (CPE) can be determined with the help of the representation below where the frequency at which the imaginary component of the impedance is considered maximum:

$$Z_{(CPE)} = \frac{1}{Q(j\omega)^n} \quad (3)$$

where $Z_{(CPE)}$ is the impedance of CPE, Q is a proportional factor, ω is the angular frequency and n is a factor which takes values between 0 and 1 indicating the inhibitor adsorption. The obtained

experimental data were fitted into Randle's equivalent circuit, as displayed in Fig. 5, to deduce the electrochemical parameters. The increased pattern of R_{ct} values obtained on addition of the extract clearly demonstrates that the system has undergone resistance towards corrosion thereby blanketing the metal surface by the added inhibitor. It is noteworthy to discuss the inhibition efficiency rendered by the extract of *Delonix elata*.

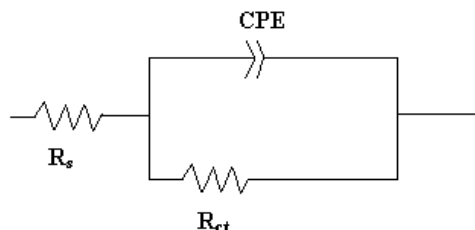


Fig. 5. Randle's equivalent circuit.

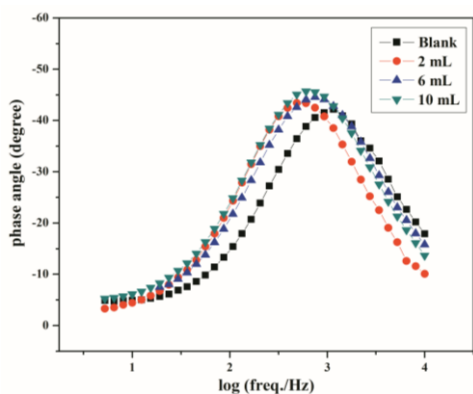


Fig. 6. Bode plot for the corrosion of mild steel in 0.5 M H₂SO₄.

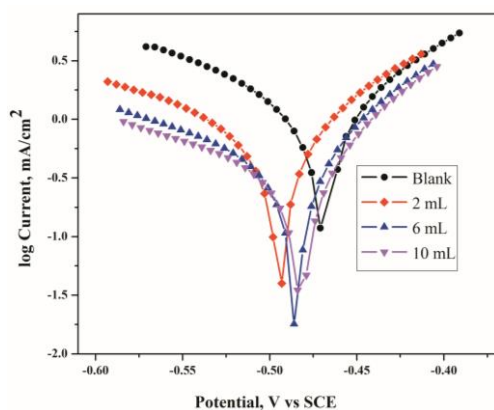


Fig. 7. Potentiodynamic polarization plot for the corrosion of mild steel in 0.5 M H₂SO₄.

Since the extract is a complex mixture of heteroaromatic compounds it is quite difficult to identify the behavior of the individual components. Thus it is assumed that all components elucidated based on their retention times could interact synergistically thereby providing a combined inhibition effect on the mild steel surface. The representation of Nyquist plot could be still better

understood by correlating Bode phase angle and modulus plot. The Bode plots shown in Fig. 6, represent the single time constant with increased phase angle for the addition of 2, 6, 10 % v/v extract compared to blank, providing a confirmation that the added extract has acted synergistically on the mild steel surface in forming a protective layer to minimize corrosion.

Potentiodynamic polarization technique

Influence of the inhibitors on the partial cathodic and anodic reaction mechanisms could be well understood with the help of potentiodynamic polarization measurements. Potentiodynamic polarization parameters such as corrosion current densities (I_{corr}), corrosion potential (E_{corr}), cathodic Tafel slope (b_c) and anodic Tafel slope (b_a) were deduced from the Tafel curves, as shown in Fig. 7 and displayed in Table 2. The obtained polarization curves show that both cathodic and anodic reactions are inhibited by the addition of inhibitors. From the parameters listed in Table 2 it could be noticed that there appears a decreased corrosion current density from 850 (blank) to 268 $\mu\text{A}/\text{cm}^2$ (inhibited) thereby minimizing the corrosion rate in the presence of inhibitors. However, the added inhibitors alter both cathodic and anodic reactions from whose curves Tafel slopes b_a and b_c could be determined. Tafel constants b_a and b_c are both affected by the addition of inhibitors, b_c to a slightly higher extent. The shifting trend in E_{corr} values was found to be 18.5 mV/sec which is less than 85 mV, suggesting mixed type of inhibition with predominant cathodic inhibition [32]. Thus, the added inhibitors can either retard cathodic hydrogen evolution or anodic dissolution of mild steel providing a mixed mode of inhibition on the mild steel surface.

Surface analysis (SEM-EDX-AFM)

Fig. 8 shows the SEM-EDX images of mild steel specimens immersed in an aggressive acid medium, as well as in a *Delonix elata* (10 % v/v) inhibited medium which confirm the formation of protective layer after immersion. The image of the blank specimen exhibited rough surface [33] with pit-like appearance confirming that the metal has undergone dissolution whereas the smooth surface shown by the inhibited specimen confirms the adsorption of phytochemical constituents on the metal surface thereby retarding corrosion. On the other hand, the corresponding EDX images shown in Fig. 8 along with the elemental composition shown in Table 3, still make the adsorption of components more precise. Comparing the images and data represented, some of the elements of lower proportion present in the blank disappeared in the

inhibited specimen giving a confirmation that the added inhibitor forms a layer on the metal surface. Additional peaks corresponding to S, N and O confirm the adsorption of multiple components of the phytochemical constituents on the metal surface where it is again a difficult task to determine the action of individual components. To study the progress of adsorption of inhibitors on the mild steel surface, AFM was used as a powerful technique nowadays which has the capability of revealing the morphology from nano to micro scale. The three-dimensional images of uninhibited and inhibited specimens are shown in Fig. 8. From the average roughness (Ra), root-mean-square

roughness (Rq), and the maximum peak-to-valley (P-V) height values obtained from AFM processing, relevant information can be secured. The obtained Ra and Rq values of (198.38 nm, 258.103 nm) blank and (80.7398 nm, 102.026 nm) for 10 % v/v inhibited plate coincided well with P-V height values of 2089.77 nm for blank and 686.106 nm for inhibited medium. All the three parameters for inhibited specimens were found to be less than those of the blank specimen, confirming the smooth surface due to the adsorption of inhibitors [33].

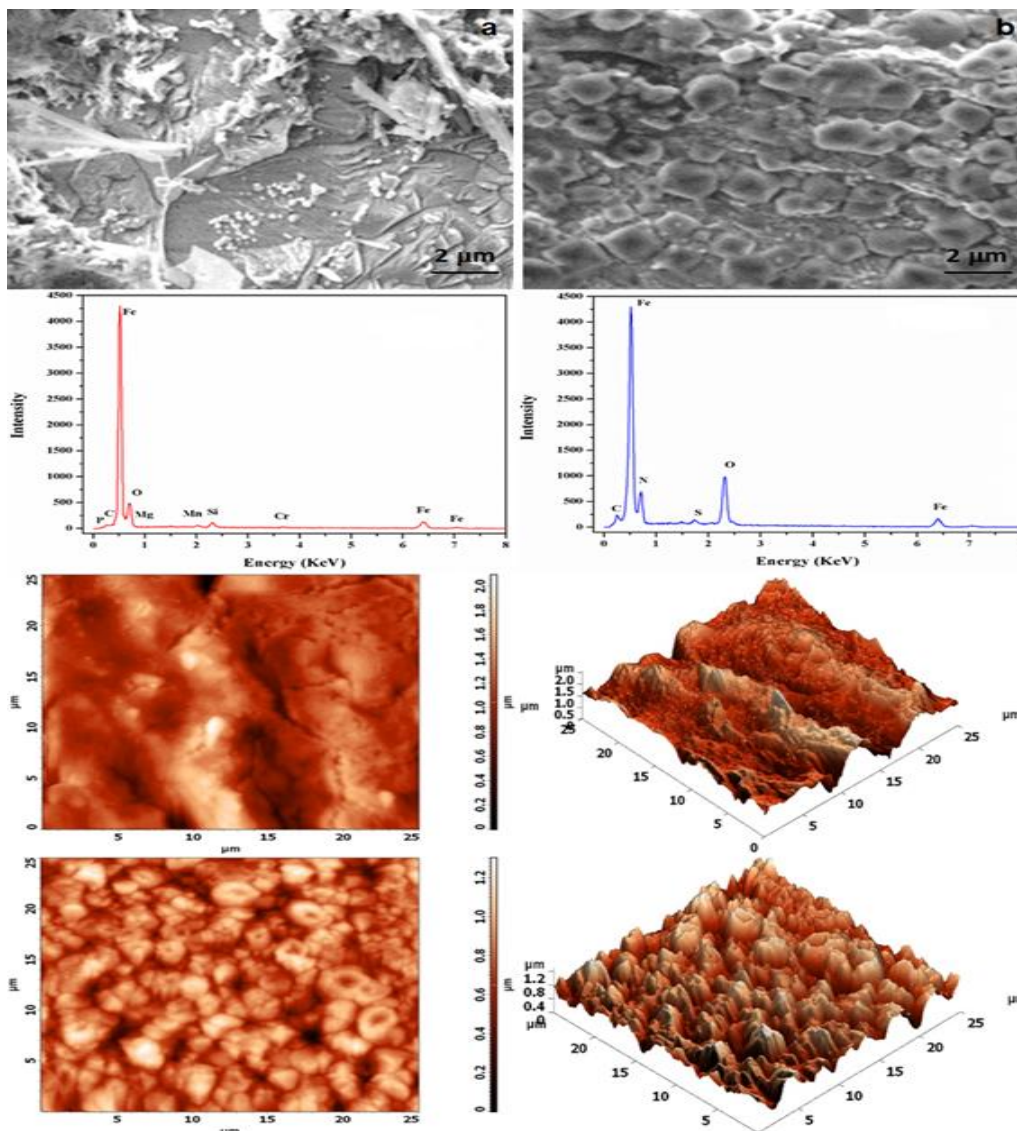


Fig. 8. SEM-EDX and AFM images of mild steel in 0.5 M H₂SO₄ a) blank, and b) 0.5M H₂SO₄ + 10% v/v *D. elata*.

Table 3. Percentage compositions of elements present on the mild steel surface.

Elements	Composition (Atomic %)	
	Blank	Inhibited
C	0.03	0.37
Fe	64.04	55.66
O	26.03	35.6
S	-	2.38
N	-	5.99
Mn	2.27	-
Cr	0.53	-
Mg	1.71	-
P	0.38	-
Si	5.01	-

CONCLUSIONS

The conclusions of the present study are as follows: (i) The phytochemical constituents of the ethanol extract of *Delonix elata* were identified by GC-MS analysis. (ii) Increased charge-transfer resistance and decreased corrosion current density were obtained from impedance and polarization techniques. Both methods correlate well with each other. (iii) The surface studies carried out using SEM, EDX, and AFM techniques confirmed the adsorption of inhibitors on the mild steel surface.

Acknowledgement: This paper was supported by the KU Research Professor Program of Konkuk University.

REFERENCES

- G. Ji, P. Dwivedi, S. Sundaram, R. Prakash, *Res. Chem. Intermed.*, **42**, 439 (2016).
- O. K. Abiola, A. O. James, *Corros. Sci.*, **52**, 661 (2010).
- E. E. Oguzie, C. K. Enenebeaku, C. O. Akalezi, S. C. Okoro, A. A. Ayuk, E. N. Ejike, *J. Colloid Interface Sci.*, **349**, 283 (2010).
- M. Prabakaran, S. H. Kim, V. Hemapriya, I. M. Chung, *J. Ind. Eng. Chem.*, **37**, 47 (2016).
- S. Bilgic, *Mater. Chem. Phys.*, **76**, 52 (2002).
- M. Gopiraman, P. Sakunthala, R. Kanmani, A. R. Vincent, N. Sulochana, *Ionics*, **17**, 843 (2011).
- R. M. A. Shahba, A. E. E. Fouda, A. E. El-Shenawy, A. S. M. Osman, *Materials Sci. Appl.*, **7**, 654 (2016).
- N. A. Odewunmi, N. A. Umoren, Z. M. Gasem, *J. Ind. Eng. Chem.*, **21**, 239 (2015).
- A.K. Satapathy, G. Gunasekaran, S. C. Sahoo, K. Amit, P. V. Rodrigues, *Corros. Sci.*, **51**, 2848 (2009).
- M. Prabakaran, S. H. Kim, K. Kalaiselvi, V. Hemapriya, I. M. Chung, *J. Taiwan Inst. Chem. Eng.*, **59**, 553 (2016).
- M. S. Nooshabadi, M.S. Ghandchi, *J. Ind. Eng. Chem.*, **31**, 231 (2015).
- L. R. Chauhan, G. Gunasekaran, *Corros. Sci.*, **49**, 1143 (2007).
- M. Prabakaran, S. H. Kim, V. Hemapriya, I. M. Chung, *Res. Chem. Intermed.*, **42**, 3703 (2016).
- M. S. A. Otaibi, M. A. Mayouf, M. Khan, S. A. A. Mazroa, H. Z. Alkhatlan, *Arabian J. Chem.*, **7**, 340 (2014).
- N. Soltani, N. Tavakkoli, M. K. Kashani, A. Mosavizadeh, E. E. Oguzie, M. R. Jalali, *J. Ind. Eng. Chem.*, **20**, 3217 (2014).
- M. A. Deyab, *J. Ind. Eng. Chem.*, **22**, 384 (2015).
- Y. Singh, E. E. Ebenso, W. Liu, J. Pan, B. Huang, *J. Ind. Eng. Chem.*, **24**, 219 (2015).
- M. G. Sethuraman, N. Sulochana, *Curr. Sci.*, **55**, 343 (1986).
- M. Vijayanthi, V. Kannan, *Afr. J. Microbiol. Res.*, **8**, 697 (2014).
- P. Krishnappa, K. Venkatarangaiyah, Venkatesh, S. K. S. Rajanna, *IJNPR*, **8**, 47 (2017).
- S. Singh, S. N. Kumar, *WJPPS*, **3**, 2042 (2014).
- M. S. Al-Otaibi, A. M. Al-Mayouf, M. Khan, A. A. Mousa, S. A. Al-Mazroa, H. Z. Alkhatlan, *Arab. J. Chem.*, **7**, 340 (2012).
- N. O. Eddy, *Portugaliae Electrochim. Acta*, **27**, 579 (2009).
- E. M. Sherif, *Int. J. Electrochem. Sci.*, **6**, 3077 (2011).
- K. M. Zohdy, *Int. J. Electrochem. Sci.*, **10**, 414 (2015).
- F. Mansfeld, *Electrochim. Acta*, **35**, 1533 (1990).
- F. Bentiss, C. Jama, B. Mernari, H. El Attari, L. El Kadi, M. Lebrini, M. Traisnel, M. Lagrenee, *Corros. Sci.*, **51**, 1628 (2009).
- N. A. Negma, N. G. Kandile, E. A. Badr, M. A. Mohammed, *Corros. Sci.*, **65**, 94 (2012).
- N. Labjar, M. Lebrini, F. Bentiss, N. E. Chihib, S. El Hajjaji, C. Jama, *Mater. Chem. Phys.*, **119**, 330 (2010).
- A.K. Singh, M. A. Quraishi, *Corros. Sci.*, **52**, 152 (2010).
- F. Bentiss, M. Traisnel, M. Lagrenee, *Corros. Sci.*, **42**, 127 (2000).
- S. B. Tutunaru, *J. Therm. Anal. Calorim.*, **127**, 863 (2016).
- P. Mourya, S. Banerjee, M. M. Singh, *Corros. Sci.*, **85**, 352 (2014).